Original Research

Study on N$_2$O Catalytic Decomposition over NiO-Mn$_2$O$_3$@SiO$_2$ Catalyst

Yuanyang Zhang[1]°*, Kun Bao[1], Wenqian Zhang[1], Yongle Zhao[1], Linqi Wang[2]

[1]School of New Materials and Chemical Engineering, Tangshan University, Tangshan 063000, China
[2]School of Artificial Intelligence, Tangshan University, Tangshan 063000, China

Abstract

A series of NiO/SiO$_2$ catalysts with different NiO loadings were first prepared using the impregnation method. The basic characterization of NiO/SiO$_2$ samples was characterized by BET and XRD. The performance of NiO/SiO$_2$ on catalytic decomposition of N$_2$O was evaluated in a fixed bed reactor, which indicated that the best performance on catalytic decomposition of N$_2$O was the sample when the loading of NiO was 16.0 (wt%), NiO(16.0%)/SiO$_2$. On this basis, a series of NiO(16.0%)-Mn$_2$O$_3$(x%)/SiO$_2$ catalysts were prepared, respectively. The experimental results showed that when the loadings of Mn$_2$O$_3$ was 6.0 (wt%), i.e., NiO(16.0%)-Mn$_2$O$_3$(6.0%)/SiO$_2$, its performance on catalytic N$_2$O decomposition was the best. The NiO (16.0%)-Mn$_2$O$_3$(x%)/SiO$_2$ samples were characterized by using XRD and H$_2$-TPR. The stability test in the laboratory fixed bed reactor lasted for 100 hours and showed that the NiO(16.0%)-Mn$_2$O$_3$ (6.0%)/SiO$_2$ catalyst had good stability for the N$_2$O catalytic decomposition, which provided the basis for further relative research.

Introduction

As early as 1997, the Kyoto Protocol specified six major greenhouse gases: carbon dioxide (CO$_2$), methane (CH$_4$), nitrous oxide (N$_2$O), hydrofluorocarbons (HFCs), perfluorocarbons (PFCs), and sulfur hexafluoride (SF$_6$), which have been included in the United Nations Framework Convention on Climate Change. Among them, N$_2$O has extremely stable properties and can exist in the atmosphere for about 150 years [1, 2]. The main hazard of N$_2$O is its destruction of the ozone layer, the formation of ozone holes, and ultimately, the greenhouse effect, which has been regarded as a major contributor to global warming and ozone layer depletion [3]. Research has shown that N$_2$O is growing at a rate of approximately 0.2-0.3% per year. Although the concentration of N$_2$O in the atmosphere is much lower than that of the greenhouse gas CO$_2$, its global warming potential (GWP) is about 310 times that of carbon dioxide, and its contribution to the greenhouse effect is about 6-10%. The emission of greenhouse gases seriously pollutes the environment, resulting in melting glaciers, rising sea levels, changes in climate zones, etc., which has led to species extinction because of the greenhouse effect. The greenhouse effect can also cause rapid changes in local weather conditions, resulting in environmental problems such as high temperatures, heat waves, tropical storms, tornadoes, etc. [4]. Consequently, addressing

---
*e-mail: yyzhang90@126.com
Tel.: +86-315-2010649
Fax: +86-315-2792159
°ORCID iD: 0000-0001-6322-7972

N$_2$O emissions has emerged as a critical research focus in efforts to mitigate its global warming potential [5].

The main sources of N$_2$O in the atmosphere are the emissions of nature and human activities; the former mainly comes from the ocean [6, 7] and natural soil [8], and the latter mainly comes from human agricultural production activities [9], fossil fuel combustion [10], industrial production emissions [11, 12], and wastewater discharge [13, 14]. The emission of N$_2$O from industrial production is about 0.9Tg/year, accounting for 15-20% of the total direct anthropogenic emissions [4, 9, 11], which mainly come from chemical production processes such as nitric acid, nylon-66, and adipic acid. Among them, the emission of N$_2$O from adipic acid plants accounts for about 70-80% of the total industrial exhaust emissions [15]. Although the proportion of N$_2$O generated from industrial exhaust to total human emissions is relatively low, with the development of industry, the demand for chemical products has gradually increased, and the proportion of N$_2$O generated from industrial exhaust to total human emissions has gradually increased. Countries around the world have been paying more and more attention to reducing N$_2$O emissions from industrial exhaust. In China's 14th Five-Year Plan of Clean and Efficient Utilization of Coal Technology, it is further required to reduce the pollutant emissions from coal combustion significantly. The value of N$_2$O emission is limited to 80 mg/Nm^3, which has not yet been met by many coal-fired power plants. It is, therefore, imperative to develop N$_2$O emission reduction technology that takes NO into account to explore a completely integrated pollutant management method [16, 17]. The chemical properties of N$_2$O are extremely stable, and how to decompose or treat it to reduce its impact on air pollution has been a research hotspot in the field of chemical engineering in recent years.

Currently, the reported N$_2$O emission reduction technologies mainly include separation and purification [15], thermal decomposition [18], selective catalytic reduction using reducing agents such as H$_2$, CH$_4$, CO, and NH$_3$ [19-22], and catalytic decomposition [23]. The cost of separation and purification technology is high, and direct thermal decomposition technology can only be achieved under high-temperature conditions, resulting in significant equipment investment. Although selective catalytic reduction could catalyze the decomposition of N$_2$O at lower temperatures, the use of some reducing agents could lead to the production of the greenhouse gas CO$_2$, which is not conducive to energy conservation and emission reduction. It is generally believed that catalytic decomposition is a promising technology for N$_2$O emission reduction. The reported catalytic decomposition methods mainly focus on precious metal catalysts [24, 25], hydrotalcite-like catalysts [26], and supported transition metal oxide catalysts [27-31]. So far, the domestic N$_2$O decomposition catalyst technology is still in the development stage, mostly in small-scale research. Therefore, developing high-performance N$_2$O decomposition catalysts to reduce

greenhouse gas emissions is of great significance for the goal of achieving a carbon peak before 2030 and carbon neutrality before 2060 in China. This article basically reported the use of the composite metal oxides of nickel and manganese supported on SiO$_2$ to achieve N$_2$O decomposition.

Materials and Methods

Materials

All of the SiO$_2$ powder, nickel (II) nitrate hexahydrate [Ni(NO$_3$)$_2$·6H$_2$O], and 50% manganese (II) nitrate aqueous solution [Mn(NO$_3$)$_2$] are analytical grade (AR) provided by Sinopharm Chemical Reagent Co., Ltd., China. Nitrogen (N$_2$) and oxygen (O$_2$) are both produced by Tangshan Zhongsheng Industrial Gas Co., Ltd., China, with a purity of 99.99 (v/v)%. Nitrous oxide (N$_2$O), produced by Luoyang Feilier Special Gas Co., Ltd., China, has a purity of 99.999 (v/v)%. The deionized water used in the experiment was prepared by using the Milli-Q ultrapure water system in the laboratory (conductivity≤0.055μS/cm).

Sample Preparation

The catalysts used in this study were prepared by the impregnation method. The SiO$_2$ used was ground and sieved to obtain a carrier with a mesh size of 40-20 (0.425-0.850 mm), which was firstly dried in a drying oven at 110-120ºC lasted for 10-12 hr. A suitable precursor aqueous solution based on the preprepared catalyst components and content was prepared, and the solution was sonicated at room temperature for 0.5-2.0 hr to ensure the formation of a uniform precursor aqueous solution before use. During the impregnation process, the prepared precursor aqueous solution was first transferred into a beaker, which was located in a constant temperature water bath at 45.0±5.0ºC; then, the prepared SiO$_2$ carrier was slowly added to the precursor solution under stirring conditions. After the SiO$_2$ carrier was completely added to the precursor solution while stirring continuously for 0.5-1.0 hr, it was filtered and dried in a drying oven at 105-110ºC for 16-24 hr. Then, the precursor catalyst was treated at 550ºC for 4-6 hr in a muffle furnace through the programmed heating method. After calcination, the sample with 40-20 mesh was collected and used to evaluate its catalytic decomposition performance of N$_2$O. The content of active components was determined by X-ray fluorescence spectroscopy (XRF) analysis.

Characterization

The specific surface area and pore structure were analyzed by using N$_2$ adsorption/desorption on a Micromeritics ASAP 2460 analyzer. X-ray fluorescence spectroscopy (XRF) was performed using a Philips

Magix PW2424 X-ray fluorescence spectrometer, and X-ray diffraction (XRD) was performed on a Rigaku SmartLab X-ray diffractometer by using CuK alpha radiation, tube voltage of 40 kV, and tube current of 100 mA. The microstructure of the photocatalyst before and after the reaction was observed using a Hitachi S-4800 scanning electron microscope (SEM) with an acceleration voltage of 5.0 kV during the imaging process. The Temperature Programmed Reduction (H$_2$-TPR) analysis was performed on an AMI-300IR fully automatic chemical adsorption instrument. 0.1 g (40-60 mesh) of catalyst was placed in a microreactor and pretreated at the temperature of 150-300ºC in an argon atmosphere for 30 min. After cooling to room temperature, it was switched to an H$_2$/Ar atmosphere as well, and the baseline stabilized. The temperature was raised to 800ºC at a rate of 10-20ºC/min. The hydrogen signal of the reaction tail gas was detected online by using a GAM 200 gas mass spectrometer (Inprocess Instruments, Germany).

Activity Evaluation

The performance of catalytic decomposition of N$_2$O was evaluated in a fixed bed reactor system, and the experimental setup is shown in Fig. 1. The reactor material was made of 310S stainless steel with an inner diameter of 8.0 mm. The outlet of the reactor was connected to a cooler, and the reaction products were condensed and entered the gas-liquid separator. The gas mixture was discharged through a back pressure valve and accumulated through a metal float flowmeter. It could be directly analyzed by gas chromatography by switching through a four-way valve. It was analyzed by using gas chromatography GC-2010 PLUS (Shimadzu), with a 5A molecular sieve and Porapak Q packed column, and a TCD detector. The conversion ratio or activity of the catalyst was calculated based on the following method.

$$N_2O \; conversion \; (\%) = (N_2O_{conversion(in)} - N_2O_{conversion(out)})/(N_2O_{conversion(in)}) \times 100\%$$

Results and Discussion

SiO$_2$-supported catalysts with different NiO contents were first prepared by using the impregnation method. The designed contents (wt) supported on SiO$_2$ were 4.0%, 8.0%, 12.0%, 16.0%, and 20.0%, respectively. X-ray fluorescence spectroscopy (XRF) results indicated that the actual loadings of NiO were 4.01%, 7.96%, 12.05%, 15.68%, and 19.69%, respectively, which was basically the designed value. In the following discussion, the loadings of NiO in the series of catalysts were based on the designed value for the reason of simplicity.

The specific surface areas of the carrier SiO$_2$ and samples of NiO(4.0%)/SiO$_2$, NiO(8.0%)/SiO$_2$, NiO(12.0%)/SiO$_2$, NiO(16.0%)/SiO$_2$, and NiO(20.0%)/SiO$_2$ were 292 m^2/g, 288 m^2/g, 280 m^2/g, 275 m^2/g, 268 m^2/g, and 259 m^2/g, respectively. It indicated that the specific surface area of the prepared NiO/SiO$_2$ catalysts gradually decreased with the increase in the content of active components on support. This could probably be because the agglomeration phenomenon of NiO on the surface of the support was gradually increasing as well, and some pores of the support were blocked with the increasing of NiO content, which resulted in a decreasing trend in specific surface area.

The XRD spectra of the prepared catalysts NiO(4.0%)/SiO$_2$, NiO(8.0%)/SiO$_2$, NiO(12.0%)/SiO$_2$, NiO(16.0%)/SiO$_2$, and NiO(20.0%)/SiO$_2$ were shown in Fig. 2, respectively. The broad diffraction peak appearing in 2θ at approximately 22º was the characteristic peak of SiO$_2$ [32], while the appearing diffraction peaks at approximately 37º, 43º, 63º, 75º, and 79º were the diffraction peaks of the face-centered cubic crystal faces (111), (200), (220), (311), and (222) of NiO (JCPDS No. 47-1049), respectively [33, 34]. Using the Scherrer
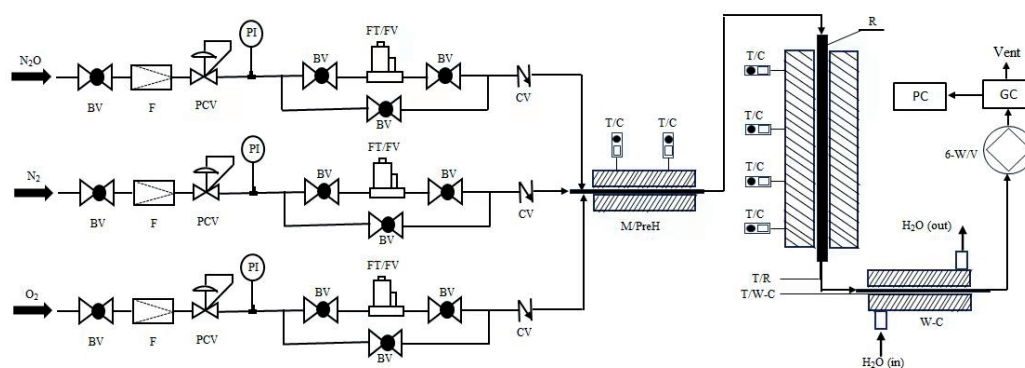

Fig. 1. The schematic diagram of the fixed bed reactor used for catalyst performance evaluation.
BV-ball valve, CV-check valve, F-filter, FT/FV-mass flow meter, GC-gas chromatography, H$_2$O(in)-condensate inlet, H$_2$O(out)-condensate outlet, M/PreH-gas mixing preheater, PC-chromatography workstation, PCV-automatic pressure reducing valve, PI-pressure sensor, R-fixed bed reactor, TC-controlled thermocouple, T/R-reactor bed temperature thermocouple, T/W-C-condenser temperature thermocouple, Vent-gas vent. W-C-water-cooled condenser, 6-W/V-gas six way valve.

formula, the average particle sizes of NiO on support for catalysts of NiO(4.0%)/SiO$_2$, NiO(8.0%)/SiO$_2$, NiO(12.0%)/SiO$_2$, NiO(16.0%)/SiO$_2$, and NiO(20.0%)/SiO$_2$ were 12.4 nm, 13.6 nm, 14.5 nm, 15.8 nm, and 16.4 nm, respectively. This indicated that the average particle size of NiO distributed on the SiO$_2$ support showed a slight increasing trend under the experimental conditions of preparation with the increasing of NiO loadings.

The conversion ratio of N$_2$O decomposition over the above prepared NiO(x%)/SiO$_2$ catalysts was shown in Fig. 3 as a function of reaction temperature. The experimental conditions are listed below: gas composition (v/v) 14.6% N$_2$O+55.2% N$_2$+30.2% O$_2$, volume space velocity of 5000 h^{-1}, and system pressure of 0.1 MPa. The experimental results showed that the activity of decomposing N$_2$O over the prepared NiO(x%)/SiO$_2$ catalysts was basically increasing with the increasing loadings of NiO on support under the experimental conditions of preparation and performance evaluation used. It showed that when the NiO loading reached 16.0 (wt%), further increasing the loadings of NiO slightly decreased its activity of the catalyst for decomposing N$_2$O, indicating that the NiO(16.0%)/SiO$_2$ catalyst had the best performance on N$_2$O decomposition under experimental conditions used with 16.0 (wt%) loadings of NiO on SiO$_2$ support.

The results of the specific surface area showed that for NiO(x%)/SiO$_2$ catalysts, as the increasing content of active component of NiO on support, the specific surface area of NiO(x%)/SiO$_2$ catalysts gradually decreased, indicating that for supported catalysts the variation of specific surface area occurring within a certain range, it did not significantly affect the activity of the catalysts
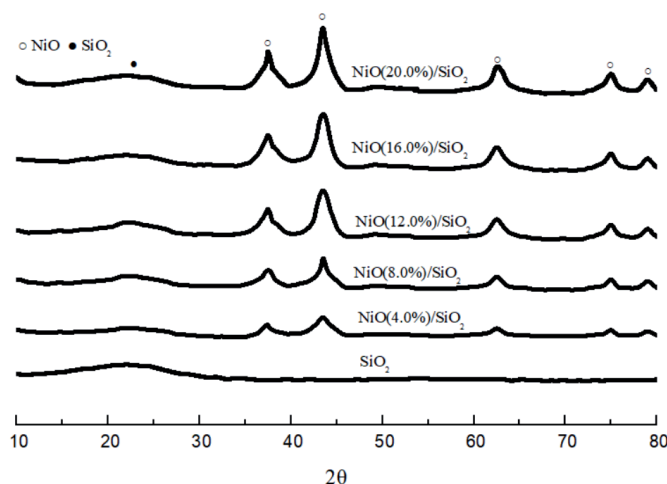

Fig. 2. XRD characterization results over NiO/SiO$_2$ samples with different NiO loadings.
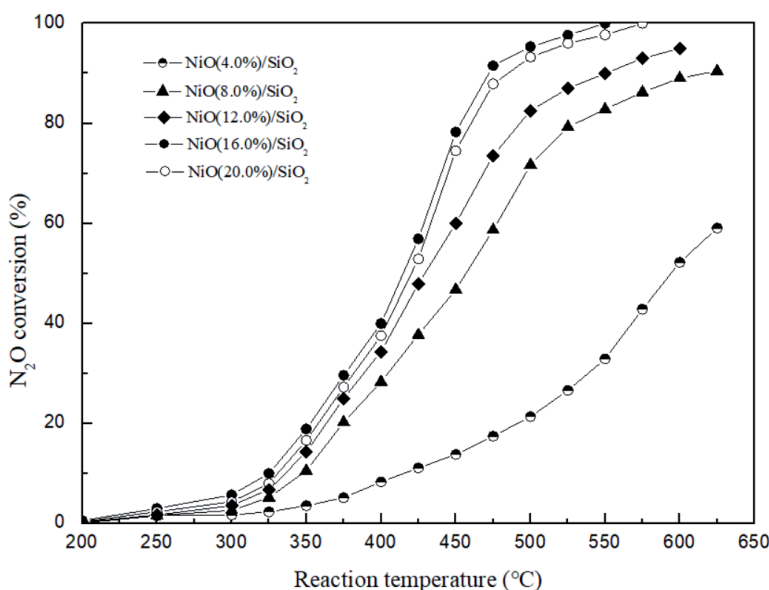

Fig. 3. The variation of N$_2$O conversion with reaction temperature on the prepared NiO(x%)/SiO$_2$ catalysts.

on N$_2$O decomposition. XRD characterization results indicated that for the NiO(x%)/SiO$_2$ catalysts when the amount of NiO loadings was relatively small, the active components were well dispersed on the support, which could fully use the catalytic function of the active components. At the same time, the amount of active component loadings would have a significant effect on the number of active centers. Taking into account the dispersion state of the active components on support and the number of active centers, the NiO(16.0%)/SiO$_2$ catalyst showed the best performance on N$_2$O decomposition under experimental conditions. The experimental results showed that under the above experimental conditions, the conversion ratio of N$_2$O on NiO(16.0%)/SiO$_2$ catalyst reached 100% when the reaction temperature was about 550ºC.

A series of NiO(16.0%)-Mn$_2$O$_3$/SiO$_2$ catalysts were prepared based on the above experimental results. The designed contents (wt) of Mn$_2$O$_3$ supported on NiO(16.0%)/SiO$_2$ were 2.0%, 4.0%, 6.0%, and 8.0%, respectively, which was basically the same as the actual value through comparing with XRF results. In the following discussion, the loadings of active components in the series of catalysts were still based on the designed value for the reason of simplicity, including NiO(16.0%)-Mn$_2$O$_3$(2.0%)/SiO$_2$, NiO(16.0%)-Mn$_2$O$_3$(4.0%)/SiO$_2$, NiO(16.0%)-Mn$_2$O$_3$(6.0%)/SiO$_2$, and NiO(16.0%)-Mn$_2$O$_3$(8.0%)/SiO$_2$, in order to further investigate the possibility of improving the activity of supported NiO/SiO$_2$ catalyst on N$_2$O decomposition. Sequentially, the specific surface areas of the prepared samples were 243 m^2/g, 238 m^2/g, 226 m^2/g, and 219 m^2/g, respectively, which indicated that the specific surface area of the prepared samples was slightly decreasing with the increase of Mn$_2$O$_3$ on NiO(16.0%)/SiO$_2$ under experimental prepared conditions, while compared with traditionally supported catalysts, the prepared samples still had relatively large specific surface area.

XRD spectra of the prepared series of samples of NiO(16.0%)-Mn$_2$O$_3$(y%)/SiO$_2$ were shown in Fig. 4,

which showed that it did not obviously appear in the characteristic peaks belonging to Mn$_2$O$_3$ on the XRD spectrum when the loading of Mn$_2$O$_3$ was 2.0% and 4.0%, respectively, which was probably because the Mn$_2$O$_3$ crystalline structure did not clearly form when the loading of Mn$_2$O$_3$ was lower under the prepared experimental conditions used. It showed two characteristic diffraction peaks at approximately 33º and 35º at 2θ when the loadings of Mn$_2$O$_3$ were 6.0% and 8.0%, respectively, which could be the diffraction peaks of Mn$_2$O$_3$ (222) and (123) crystal planes (JCPDF No. 78-0390), respectively [35,36].

In order to investigate the ability of reduction for the prepared NiO-Mn$_2$O$_3$@SiO$_2$ samples, H$_2$-TPR performance performed on the prepared series of catalysts of NiO(16.0%)-Mn$_2$O$_3$(y%)/SiO$_2$ was tested, and results were shown in Fig. 5, respectively. The results showed that there were mainly two H$_2$-TPR hydrogen consumption peaks at approximately 300-470ºC and 510-620ºC for the catalysts of NiO(16.0%)-Mn$_2$O$_3$(y%)/SiO$_2$ with different loadings, respectively. The hydrogen consumption peak at a low temperature of 300-470ºC could be attributed to the weak interaction between NiO and the support of SiO$_2$ in the free state of NiO, while the hydrogen consumption peak at a high temperature of 510-620ºC could be attributed to the strong interaction between NiO and the support of SiO$_2$, respectively [37].

The peak area related to the hydrogen consumption at low-temperature (300-470ºC) (A1) and high-temperature (510-620ºC) (A2) were calculated, respectively, by using Origin peak integration (Table 1). It showed that the peak area of hydrogen consumption (A1) and (A2) both increased with the increasing content of Mn$_2$O$_3$ with the loading of Mn$_2$O$_3$ (wt%)≤6.0%, indicating that the ability to reduce for the catalysts increased with the increasing content of Mn$_2$O$_3$. However, it showed that the peak area of hydrogen consumption (A1) and hydrogen consumption (A2) was actually decreased when the content of Mn$_2$O$_3$ (wt%) was higher than that of 6.0%,
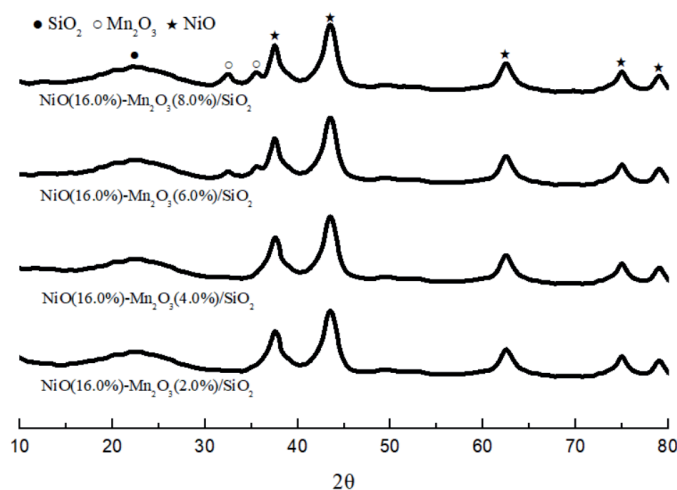

Fig. 4. XRD characterization results over NiO(16.0%)-Mn$_2$O$_3$/SiO$_2$ samples with different Mn$_2$O$_3$ loadings.

Table 1. The peak area of hydrogen consumption for H_2-TPR over NiO and NiO-Mn_2O_3@SiO_2 catalysts.
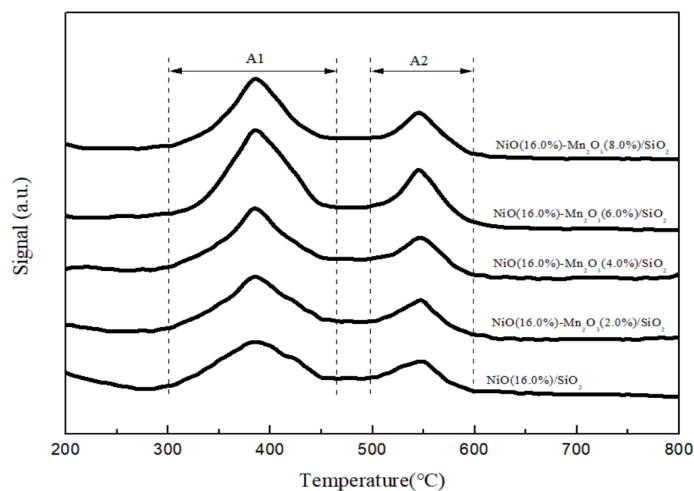
Samples	Relative peak area (a.u.)	
	A1(300~470ºC)	A2(510~620ºC)
NiO(16.0%)/SiO$_2$	507.54	95.27
NiO(16.0%)-Mn$_2$O$_3$(2.0%)/SiO$_2$	600.90	185.11
NiO(16.0%)-Mn$_2$O$_3$(4.0%)/SiO$_2$	657.20	247.14
NiO(16.0%)-Mn$_2$O$_3$(6.0%)/SiO$_2$	980.14	485.16
NiO(16.0%)-Mn$_2$O$_3$(8.0%)/SiO$_2$	820.36	440.86

indicating that the ability to reduce for the catalyst was decreased with the further increasing the content of Mn_2O_3 when the content of Mn_2O_3 was higher than that of 6.0%. This implied that the sample of NiO(16.0%)-Mn_2O_3(6.0%)/SiO_2 had the best ability of reduction for the prepared catalysts of NiO(16.0%)-Mn_2O_3(y%)/SiO_2 under the experimental preparation conditions used. For N_2O decomposition catalysts, research results have shown that the stronger the ability to reduce, the higher the catalytic decomposition activity of N_2O under certain experimental conditions [19, 23].

Fig. 6 shows the experimental results of the N_2O conversion over the prepared catalysts of NiO(16.0%)-Mn_2O_3(y%)/SiO_2 as the function of reaction temperature. The experimental conditions are listed below: gas composition (v/v) 14.6% N_2O+55.2% N_2+30.2% O_2, volume space velocity of 5000 h^{-1}, and system pressure of 0.1 MPa, respectively. It indicated that the catalytic activity performing on N_2O decomposition was improved to some degrees under experimental conditions for the supported catalysts of composite NiO-Mn_2O_3 metal oxides, NiO(16.0%)-Mn_2O_3(y%)/SiO_2 under experimental condition. Rational design of bimetallic catalysts has progressed in recent studies owing to the understanding of synergy and strong mutual interaction between metal oxide species [38].

The theoretical analysis results of the relationship between the ionization potential (ev) and the ratio of effective nuclear charge/ion radius for the representative oxides of transition and alkali metals indicated that NiO and Mn_2O_3 belong to alkaline oxides and amphoteric metal oxides, respectively [39]. Further research showed that the catalytic performance of composite metal oxides prepared by doping modification of alkaline metal oxides with amphoteric metal oxides was better than that of single alkaline metal oxides or amphoteric metal oxides [40, 41]. Meanwhile, according to the mechanism of N_2O catalytic decomposition [42, 43], the desorption of O* on the active sites (*) from the catalyst surface would play an important role in the catalytic decomposition of N_2O, while the surface of Mn_2O_3 metal oxide could provide abundant of O active sites. Therefore, the catalysts of NiO-Mn_2O_3/SiO_2 prepared under experimental conditions would have better performance on N_2O decomposition than that of NiO/SiO_2 catalysts, which was basically consistent with the experimental results (Fig. 6).

The experimental results in Fig. 6 also indicated that the activity of the prepared NiO(16.0%)-Mn_2O_3(y%)/SiO_2 catalyst performing on N_2O decomposition was increased with the increasing of Mn_2O_3 content when the content of Mn_2O_3 was lower than that of 6.0 (wt%), while

Fig. 5. H_2-TPR characterization results over NiO(16.0%)-Mn_2O_3/SiO_2 samples with different Mn_2O_3 loadings.
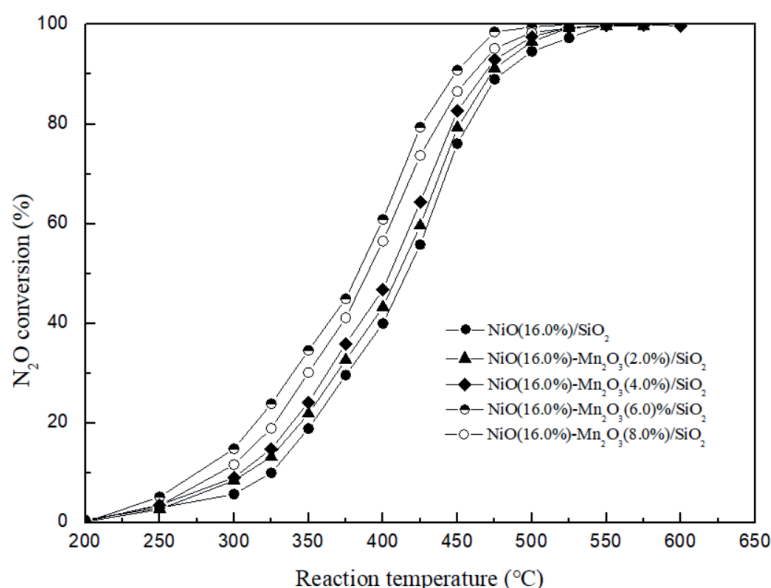
Fig. 6. The variation of N_2O conversion with reaction temperature on the prepared $NiO(16.0\%)-Mn_2O_3(y\%)/SiO_2$ catalysts.

the activity of the prepared $NiO(16.0\%)-Mn_2O_3(y\%)/SiO_2$ catalyst performing on N_2O decomposition was decreased with the increasing of Mn_2O_3 content when the content of Mn_2O_3 was higher than that of 6.0 (wt%), indicating that it existed an appropriate composition ratio for the synergistic catalytic function between the composite metal oxides of $NiO-Mn_2O_3$. Under the experimental preparation conditions, the catalyst prepared for $NiO(16.0\%)-Mn_2O_3(6.0\%)/SiO_2$ showed the best activity in N_2O decomposition. At the reaction temperature of 525ºC and other experimental conditions used, the conversion of N_2O over the catalyst of $NiO(16.0\%)-Mn_2O_3(6.0\%)/SiO_2$ was 100%, which was consistent with the H_2-TPR characterization results. Under the same experimental conditions used, the conversion of N_2O over the catalyst of $NiO(16.0\%)/SiO_2$

reached 100% at the reaction temperature of 550ºC. The stability test in the laboratory fixed bed reactor lasted for 100 hr under the following experimental conditions: gas composition (v/v) 14.6% N_2O+55.2% N_2+30.2% O_2, volume space velocity of 5000 h^{-1}, system pressure of 0.1 MPa, and reaction temperature of 525ºC. It showed that the $NiO(16.0\%)-Mn_2O_3$ (6.0%)/ SiO_2 catalyst had good stability for the N_2O catalytic decomposition, and the conversion ratio of N_2O was 100% under the experimental conditions used. Fig. 7 showed SEM characterization results of $NiO(16.0\%)-Mn_2O_3(6.0\%)/SiO_2$ catalyst before and after the reaction lasted for 100 hours, which indicated that there was no significant variation regarding the surface morphology and particle size of the catalyst before and after the reaction, respectively, which also indicated that
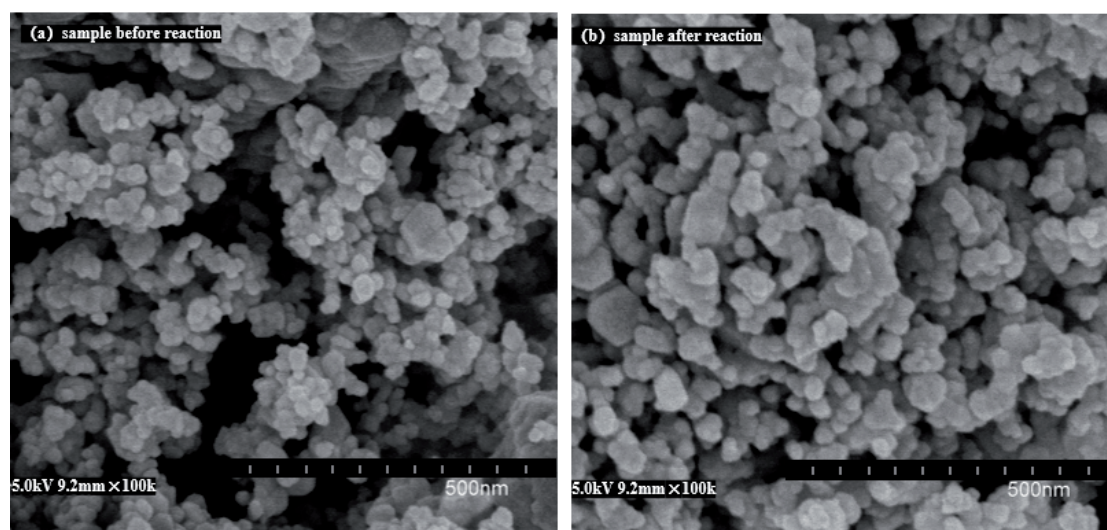

Fig. 7. SEM characterization over samples before and after the reaction lasted for 100 hours.

the prepared sample had good stability for the N_2O catalytic decomposition and provided the basis for further relative research.

Conclusions

The activity results performed on NiO(x%)/SiO_2 catalysts showed that under experimental conditions, when the content of NiO was 16.0 (wt%), NiO(16.0%)/SiO_2 had good performance over N_2O decomposition. Based on this basis, NiO(16.0%)-Mn_2O_3(x%)/SiO_2 catalysts were prepared, respectively. H_2-TPR characterization results showed that when the content of Mn_2O_3 content was 6.0 (wt%), NiO(16.0%)-Mn_2O_3(6.0%)/SiO_2, it exhibited the best reduction performance through H_2-TPR. It showed that the prepared catalyst of NiO(16.0%)-Mn_2O_3(6.0%)/SiO_2 had the best activity in N_2O decomposition among catalysts of NiO(16.0%)-Mn_2O_3(x%)/SiO_2. At the reaction temperature of 525ºC and other experimental conditions used, the conversion of N_2O reached 100% for the catalyst of NiO(16.0%)-Mn_2O_3(6.0%)/SiO_2, which was consistent with the H_2-TPR characterization results, while under same experimental conditions used, the conversion of N_2O over the catalyst of NiO(16.0%)/SiO_2 reached 100% at the reaction temperature of 550ºC. The experimental results showed that the activity of the composite metal oxides of the NiO-Mn_2O_3/SiO_2 catalyst was superior to that of the single component of the NiO/SiO_2 catalyst.

Acknowledgments

Conflict of Interest

The authors declare no conflict of interest.

References

1. ZHANG Y.Y., GUO Y.Q., LI N., FENG Y.Y. Research status and progress on N_2O abatement and recycling technique N_2O. Environmental Protection of Chemical Industry. **38** (1), 499, **2018**.
2. YUAN C.J. Nitrous Oxide: Laughing gas should not be laughed off. Huaxue Tongbao. **86** (2), 244, **2023**.
3. LI A Q., WANG P., ZHANG L.D., ZHAO H.Y., JIN M.M., LEI L.L. Effect of different skeleton structures on N_2O decomposition from ammonia-fueled engines using Fe-based zeolite catalysts. Fuel. **378**, 132888, **2024**.
4. CHIPPERFIELD M.P., BEKKI S., DHOMSE S., HARRIS NEIL R.P., HASSLER B., HOSSAINI R., STEINBRECHT W., THIÉBLEMONT R., WEBER M. Detecting recovery of the stratospheric ozone layer. Nature. **549** (7671), 211, **2017**.
5. ZHAO H.Y., WANG P., LI Z.L., AO C.C., ZHAO X.T., LIN H. Improved activity and significant O_2 resistance of Cs doped Co_3O_4 catalyst for N_2O decomposition. Journal of Environmental Chemical Engineering. **12** (5),113907, **2024**.
6. GONÇALVES C., NOGUEIRA M., OLIVEIRA A. Greenhouse gas (N_2O) emission from Portuguese estuaries. Conference: IMMR, International Meeting on Marine Research 2014 , Peniche, Portugal. Frontiers in Marine Science. **2014**.
7. YANG F., MIAO Y.Q., YE A.Z., CUI Q., SUN Y.L., LUO H., HONG W.L., SUN F.H. Characterization of N_2O emission at the water-gas interface and influence of Lake Chaohu. Journal of Lake Science. **35** (6), 2000, **2023**.
8. HUANG Y.H., SHE D.L., SHI Z.Q., HU L., PAN Y.C. Effect of different soil salinities on N_2O emission: A meta-analysis. Environmental Science. **45** (4), 1, **2023**.
9. TANG H.B., LÜ X.H., LI F.S., ZHAO S.T. Characteristics of greenhouse gas emissions in global food system. Research of Environmental Sciences. **36** (11), 1, **2023**.
10. LIU J.X., WANG X.C., LI C.Q., WANG H., SONG Y.J. Research progresses of metal oxide catalysts for direct catalytic decomposition of nitrous oxide. Environmental Protection of Chemical Industry. **41** (3), 263, **2021**.
11. JIA G.W., YANG N., WU X.H. The situation and suggestions for the control of non-carbon dioxide greenhouse gas emissions in China. Environmental Impact Assessment. **45** (3), 1, **2023**.
12. ZHANG C.H., YAO X. Path analysis and development trend of greenhouse gas treatment in tail gas of adipic acid industrial production. Henan Chemical Industry. **39** (9), 12, **2022**.
13. WANG C.X., LI Y.K., LIU Y.C. Effect of modified biochar on the removal of nitrate with low concentration and N_2O emission from water by a screened denitrifying bacterium. China Environmental Science. https://doi.org/10.19674/j.cnki.issn1000-6923.20230802.006. **2023** [In Chinese].
14. WENG J.Y., XU R.Z., YANG J., CHEN L.L., FANG F. Current status and prospects of nitrogen oxides reduction and resource utilization in wastewater treatment systems. Applied Chemical Industry. **52** (9), 2637, **2023**.
15. JIN D.X., LI S.F., PU R.J., HE Z.Y., JIANG G.Z., ZHANG F.J., LI G.Y., LU X.H., LI X.J., PU B.L. Method for recovering and purifying nitrous oxide from a gas mixture containing nitrous oxide. Chinese Patent 109476483A [P]. **2019** [In Chinese].
16. MIAO M., ZHOU T., WANG T., LI C.R., ZHANG M., YANG H.R. Feasibility of using red mud as bed material for treating N_2O in fluidized bed combustion. Fuel. **379**, 133068, **2025**.
17. LIU H., YANG S., MI J.X., SUN C.Z., CHEN J.J., LI J.H. 4d-2p-4f gradient orbital coupling enables tandem catalysis for simultaneous abatement of N_2O and CO on atomically dispersed Rh/CeO_2 catalyst. Environmental Science & Technology. **58** (38): 17125, **2024**.
18. ZHANG D.Z., ZHAO Z., ZHANG C.H., LIU Z.J., TIAN Y.F., ZHONG R.X., LI Z.G., LI X.Y., YAO X., SONG M.M., FENG X., ZHAO X.W., LIU W., ZHANG S.W., SU Y.H. A high-temperature decomposition device and method for industrial exhaust gas containing N_2O. Chinese Patent 114754363A [P]. **2022**.
19. ZHAO F.L., ZENG J., XIAO R., QIU L., GUO W., CHEN H.H., CHANG H.Z. Selective catalytic reduction

of N_2O by CO over lanthanum doped Fe-beta zeolite. China Environmental Science. **43** (3), 1044, **2023**.

20. MAUVEZIN M. Catalytic reduction of N_2O by NH_3 in presence of oxygen using Fe-exchanged zeolites. Catalysis Letters. **62** (1), 41, **1999**.

21. KAMEOKA S., SUZUKI T., YUZAKI K., TAKEDA T., TANAKA S. Selective catalytic reduction of N_2O with methane in the presence of excess oxygen over Fe-BEA zeolite. Chemical communications. **9**, 745, **2000**.

22. ZENG J., CHEN S.Y., FAN Z.H., WANG C., LI J. Simultaneous selective catalytic reduction of NO and N_2O by NH_3 over Fe-zeolite catalysts. Industrial & Engineering Chemistry Research. **59** (44), 19500. **2020**.

23. SÁDOVSKÁ G., TABOR E., SAZAMA P., LHOTKA M., SOBALÍK Z. High temperature performance and stability of Fe-FER catalyst for N_2O decomposition. Catalysis Communications. **89**, 133, **2017**.

24. ZHANG Y.Y., GUO Y.Q., LI N., FENG Y.Y. Catalytic decomposition of N_2O over supported RuO2/MexOy (Me=La, Mg, Al) catalysts. Industrial Catalysis. **26** (7), 43, **2018**.

25. CHATZIIONA V.K., CONSTANTINOU B.K., SAVVA P.G., OLYMPIOU G.G., KAPNISIS K., ANAYIOTOS A., COSTA C.N. Regulating the catalytic properties of Pt/Al_2O_3 through nanoscale inkjet printing. Catalysis Communications. **103**, 69, **2018**.

26. ZHANG Y.Y., GUO Y.Q., LI N., FENG Y.Y. The preparation of hydrotalcite-like composite metal oxides and investigation on N_2O catalytic decomposition. Environmental Pollution & Control. **41** (5), 510, **2019**.

27. CAMPA M.C., PIETROGIACOMI D., TUTI S.C., LEA R., OCCHIUZZI M. N_2O decomposition on CoO_x, CuO_x, FeO_x or MnO_x supported on ZrO_2: The effect of zirconia doping with sulfates or K^+ on catalytic activity. Applied Catalysis B: Environmental. **187** (15), 218, **2016**.

28. YU H.B. WANG X.P. Apparent activation energies and reaction rates of N_2O decomposition via different routes over Co_3O_4. Catalysis Communications. **106**, 40, **2018**.

29. SUN J.R., XIA L., LI J.Y., LI S.X., LIU X.G., WANG H., LI C.Q., SONG Y.J. Effect of crystallization temperature on catalytic performance of Co_3O_4 catalysts in decomposition of N_2O. Modern Chemical Industry. **39** (4), 89, **2019**.

30. JIA R., DONG W.Y., ZHANG L., YU H.B., JIANG X., ZHANG H.Z., LI S.J., QU M.H. Catalytic decomposition of N_2O over Co_3O_4/KIT-6 catalyst. Journal of Molecular Science. **39** (2), 154, **2023**.

31. WANG Y.F., WANG Y.T., WANG X.C., MA X.F., LI C.Q., WANG H., SONG Y.J. Study on catalytic decomposition of N_2O by SiO_2 aerogel supported transition metal oxides. Modern Chemical Industry. **42** (9), 134, **2022**.

32. CUI Y., LIN Y.B. Preparation and properties study on magnetic nanosilicon dioxide. Journal of Changchun University of Science and Technology (Natural Science Edition). **39** (6), 53, **2016**.

33. ZHOU H., LV B.L., XU Y., WU D. Synthesis and electrochemical properties of NiO nanospindles. Materials Research Bulletin. **50**, 399, **2014**.

34. YANG P., WEI X.W., WANG J., YANG F., ZHENG X.Y. Research on oxidation mechanism and fabrication of nickel oxide nanowires via high temperature oxidation. Journal of Xihua University (Natural Science). **34** (3), 70, **2015**.

35. XIA H.Y., HU L., YAO Q.Z. Preparation and photocatalytic activity of Mn_2O_3 microspheres. Journal of Inorganic Materials. **26** (3), 317, **2011**.

36. LIN Y.L., WU F., XIE Z.J., GAO B., TANG M., LU Y.N., WANG Y.C., ZHANG S., LIU Y.H., LIU Y.H. High Temperature crystallization synthesis $Mn_2O_3@MoS_2$ composite materials and their adsorption properties for Uranium. Journal of Nuclear and Radiochemistry. **44** (4), 457, **2022**.

37. ZHAO D., TAN J.S., JI Q.Q., ZHANG J.T., ZHAO X.S., GUO P.Z. Mn_2O_3 nanomaterials: Facile synthesis and electrochemical properties. Chinese Journal of Inorganic Chemistry. **26** (5), 832, **2010**.

38. LIU L.J., LIU B., NAKAGAWA Y., LIU S.B., WANG L., YABUSHITA M., TOMISHIGE K. Recent progress on bimetallic catalysts for the production of fuels and chemicals from biomass and plastics by hydrodeoxygenation. Chinese Journal of Catalysis. **62** (7), 1, **2024**.

39. ZHANG Y.Y. Catalytic decomposition of greenhouse gas N_2O – Investigation on preparation and performance of composite metal oxide catalysts [D]. East China University of Science and Technology. **2000**.

40. HUANG Q.X., WANG F., LIU Y., ZHANG B.Y., GUO F.Y., JIA Z.Q., WANG H., YANG T.X., WU H.T., REN F.Z., YI F.F. Recent progress of two-dimensional metal-base catalysts in urea oxidation reaction. Rare Metals. **43** (8):3607, **2024**.

41. VASAVAN H.N., BADOLE M., SAXENA S., SRIHARI V., DAS A.K., GAMI P., DAGAR N., DESWAL S., KUMAR P., POSWAL H.K., KUMAR S. Identification of optimal composition with superior electrochemical properties along the zero Mn^{3+} line in $Na_{0.75}(Mn\text{-}Al\text{-}Ni)O_2$ pseudo ternary system. Journal of Energy Chemistry. **96** (9), 206, **2024**.

42. LIU Z., ZHOU Z., HE F., CHEN B., ZHAO Y., XU Q. Catalytic decomposition of N_2O over $NiO\text{-}CeO_2$ mixed oxide catalyst. Catalyst Today. **293-294**, 56, **2017**.

43. FRANKEN T., PALKOVITS R. Investigation of potassium doped mixed spinels $Cu_xCo_{3-x}O_4$ as catalysts for an efficient N_2O decomposition in real reaction conditions. Applied Catalysis B: Environmental. **176-177**, 298, **2015**.